AIP | Applied Physics Letters

Compositional dependence of the band-gap of Ge1−x−ySixSny alloys

Torsten Wendav, Inga A. Fischer, Michele Montanari, Marvin Hartwig Zoellner, Wolfgang Klesse, Giovanni Capellini, Nils von den Driesch, Michael Oehme, Dan Buca, Kurt Busch, and Jörg Schulze

Citation: Applied Physics Letters **108**, 242104 (2016); doi: 10.1063/1.4953784
View online: http://dx.doi.org/10.1063/1.4953784
View Table of Contents: http://scitation.aip.org/content/aip/journal/apl/108/24?ver=pdfcov
Published by the AIP Publishing

Compositional dependence of the band-gap of $Ge_{1-x-y}Si_xSn_y$ alloys

Torsten Wendav,[1,a)] Inga A. Fischer,[2] Michele Montanari,[3] Marvin Hartwig Zoellner,[3] Wolfgang Klesse,[3] Giovanni Capellini,[3,4] Nils von den Driesch,[5] Michael Oehme,[2] Dan Buca,[5] Kurt Busch,[1,6] and Jörg Schulze[2]
[1]*AG Theoretische Optik & Photonik, Humboldt Universität zu Berlin, Newtonstr. 15, 12489 Berlin, Germany*
[2]*Institut für Halbleitertechnik, Universität Stuttgart, Pfaffenwaldring 47, 70569 Stuttgart, Germany*
[3]*IHP, Im Technologiepark 25, 15236 Frankfurt (Oder), Germany*
[4]*Dipartimento di Scienze, Università Roma Tre, Viale Marconi 446, 00146 Roma, Italy*
[5]*Peter Grünberg Institute 9 (PGI 9) and JARA-Fundamentals of Future Information Technologies, Forschungszentrum Jülich, 52428 Jülich, Germany*
[6]*Max-Born-Institut, Max-Born-Str. 2 A, 12489 Berlin, Germany*

(Received 6 March 2016; accepted 31 May 2016; published online 14 June 2016)

The group-IV semiconductor alloy $Ge_{1-x-y}Si_xSn_y$ has recently attracted great interest due to its prospective potential for use in optoelectronics, electronics, and photovoltaics. Here, we investigate molecular beam epitaxy grown $Ge_{1-x-y}Si_xSn_y$ alloys lattice-matched to Ge with large Si and Sn concentrations of up to 42% and 10%, respectively. The samples were characterized in detail by Rutherford backscattering/channeling spectroscopy for composition and crystal quality, x-ray diffraction for strain determination, and photoluminescence spectroscopy for the assessment of band-gap energies. Moreover, the experimentally extracted material parameters were used to determine the SiSn bowing and to make predictions about the optical transition energy. *Published by AIP Publishing.* [http://dx.doi.org/10.1063/1.4953784]

The need for CMOS integrable and energy efficient photonic devices has driven the development of novel group-IV materials such as binary GeSn and ternary GeSiSn alloys, looking not only for the missing property in the Si group, the direct band-gap, but also for novel heterostructures with improved functionalities. While Ge[1] and GeSn[2] alloys were demonstrated to be feasible optically active media, GeSiSn alloys, due to the possibility to tune band-gap energy and lattice constant independently, may serve as natural barrier material in Ge/GeSiSn and GeSn/GeSiSn quantum well structures.[3–6] The very same material property makes it also attractive for the use in multi-junction solar cells as well as in tunneling field effect transistors (TFETs).[7,8] However, the electronic properties of the $Ge_{1-x-y}Si_xSn_y$ alloys are far from being known, in particular, at relatively high Si and Sn concentrations. The gap energy at the Γ-point (referred to in the following as direct band-gap) is suggested to depend linearly on the Si and Sn concentrations for $x + y < 0.5$ only,[9] while for higher concentrations the direct band-gap bowing parameters b of the binary alloys SiGe, GeSn, and SiSn have to be included, leading to the semi-empirical relationship:[10]

$$E_g(x,y) = E_g^{Ge}(1-x-y) + E_g^{Si}x + E_g^{Sn}y - b^{SiGe}x(1-x-y) - b^{GeSn}(1-x-y)y - b^{SiSn}xy. \quad (1)$$

While the SiGe and GeSn bowing parameters are known,[11,12] the experimental determination of b^{SiSn} values is more challenging owing to the large lattice mismatch between silicon and tin which hinders the growth of high quality SiSn alloys.[13] To date, no systematic experimental study on the bowing parameter of SiSn binary alloys has been reported. D'Costa *et al.*[14] deduced a bowing parameter of $b^{SiSn} = 13.2$ eV from experimental studies on ternary $Ge_{1-x-y}Si_xSn_y$ alloys lattice-matched to Ge, whereas Lin *et al.*[15] found $b^{SiSn} = -21$ eV for $Ge_{1-x-y}Si_xSn_y$ alloys with a lattice constant different from Ge. The theoretical value predicted by Moontragoon *et al.*,[16] which covers the entire range of concentrations, lies somewhere in between at $b^{SiSn} = 3.92$ eV, whereas Sant and Schenk[17] predicted a value of $b^{SiSn} = -5.95$ eV. This large uncertainty in the bowing parameter of SiSn makes predictions of the optical properties of $Ge_{1-x-y}Si_xSn_y$ ternary alloys difficult. In order to address this issue, we present a photoluminescence study on the $Ge_{1-x-y}Si_xSn_y$ alloys with lattice constants close to Ge. We extend the analysis to GeSiSn-alloys-composition ranges not reached to date by incorporation of up to 42% Si.

The $Ge_{1-x-y}Si_xSn_y$ layers were deposited by means of solid-source MBE on 4 in. substrates. Fluxes of the Sn and Ge effusion cells as well as of the Si electron beam evaporator were calibrated separately and adjusted to obtain a total growth rate of 1 Å/s. The sample growth started with 50 nm of Si (buffer layer) at 600 °C to improve the 4 in. Si(001) substrate quality after the *in-situ* epi-cleaning process. A 100 nm-thick layer of Ge was then deposited at a substrate temperature of 330 °C followed by an annealing step at 810 °C to form a virtual substrate (VS) for subsequent epitaxial growth of high-quality relaxed $Ge_{1-x-y}Si_xSn_y$ layers. On this virtual substrate, a 100 nm-thick $Ge_{1-x-y}Si_xSn_y$ layer was grown at a substrate temperature of 160 °C. Two selected samples are discussed here. The (Si, Sn) nominal composition of (19 at. %, 5 at. %) and (42 at. %, 10 at. %), in the following referred to as sample A and sample B, respectively, was chosen such that the GeSiSn alloys are lattice-matched to the Ge-VS (see Table I). The samples were characterized using Rutherford backscattering spectrometry (RBS), x-ray diffraction (XRD), and μ-photoluminescence spectroscopy (μPL).

a)wendav@physik.hu-berlin.de

TABLE I. Material concentrations according to RBS measurements performed at the middle of the wafer, the edge, and an intermittent position. Also displayed is the average value of all positions compared to the nominal concentrations (given in parentheses).

Sample A	%Si	%Ge	%Sn
Middle	18.5	76.0	5.5
Intermittent	19.3	75.0	5.7
Edge	19.5	74.3	6.2
Mean	19.1 (18)	75.1 (77)	5.8 (5)
Sample B	%Si	%Ge	%Sn
Middle	41.8	49.5	8.7
Intermittent	41.8	49.2	9.0
Edge	42.2	48.0	9.8
Mean	41.9 (37)	48.9 (53)	9.2 (10)

RBS measurements were performed employing 1.4 MeV $He+$ ions from a Tandetron accelerator at a back scattering angle of 170° in both random and crystal channeling modes. Fitting of the random spectra was performed using the RUMP simulation software, which yields stoichiometric information within an error of less than 0.5%.

For each sample, RBS measurements were performed at three distinct positions: at the center of the wafer, at the edge, and intermittently. Representative RBS plots for sample A and sample B are shown in Figure 1. The minimum channeling yield, defined as the ratio between channeling and random spectra directly behind the surface peak, was measured to have the rather low value of 6% (12%) for sample A (sample B) indicating a high atom-substitutionality in the epi-layer.

The measured compositions show a gradient of roughly 1% from the center of the wafer to the edge due to the asymmetric position of the material sources (see Table I). From the comparison of measured material concentration and indicated nominal values, we find a deviation of the mean tin (silicon) concentration from the nominal value of at most 1% (5%). The thickness variation of the $Ge_{1-x-y}Si_xSn_y$ layers as extracted by RBS is ±3 nm across the wafer. The uniformity of the deposition in the circumferential direction has been confirmed by measurements not reported here.

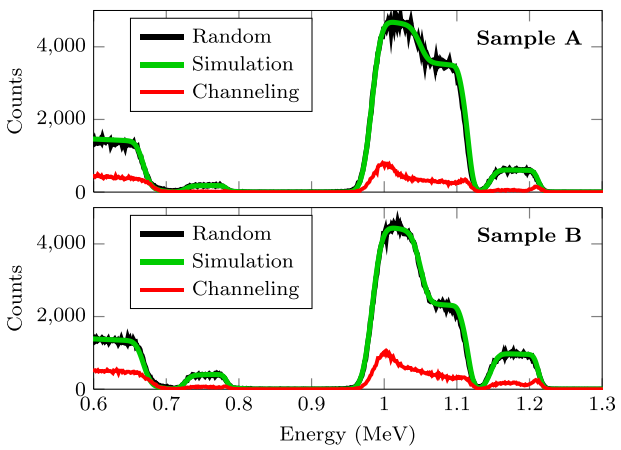

FIG. 1. Representative plot of the RBS data (black), simulation (green), and channeling (red) recorded at the center of wafer for sample A (top) and sample B (bottom).

The XRD measurements were performed with a SmartLab diffractometer from Rigaku using CuKα radiation. For the reciprocal space mappings (RSM), a high-resolution setup in line-focus geometry was used with a channel-cut Ge (400 × 2) beam collimator and a Ge (220 × 2) analyzer crystal.

Figure 2 shows the RSM of our samples around the (224) Bragg reflection of Ge and $Ge_{1-x-y}Si_xSn_y$. The position of the Ge peak reveals a tensile strain of the Ge VS of $\epsilon = 0.21\%$ for both samples which was introduced by the growth process due to the different coefficients of thermal expansion.[19] From the vertical alignment of the Ge and $Ge_{1-x-y}Si_xSn_y$ Bragg reflections, it can be seen that both samples are pseudomorphically grown on the Ge VS. The net strain of the $Ge_{1-x-y}Si_xSn_y$ layers, compared to the unstrained material, is tensile for both samples with $\epsilon = 0.09\%$ ($\epsilon = 0.56\%$) for sample A (sample B). Using the measured parallel and perpendicular lattice constants of the two samples together with the linearly averaged elastic constants of the constituent materials, we calculated the lattice constant of the unstrained alloy by a biaxial strain model.[20] We compared this value to the value we obtain when applying Vegard's law to the lattice constants of the elemental semiconductors as well as to the empirical relation suggested in Ref. 18 for the lattice constant of the ternary alloy (see Table II). Even though the relative difference for both approaches is less than 1%, we find that the prediction made with Vegard's law lie within the experimental uncertainties of the XRD measurements (0.006 Å) whereas the predictions made following the empirical relationship of Ref. 18 lie outside the interval of experimental uncertainty.

The μPL measurements were carried out using a custom-designed Horiba setup featuring a 50× optical microscope (numerical aperture A = 0.65), a high resolution spectrometer optimized for IR measurements (Horiba iHR320), an extended-InGaAs detector (0.6 eV–1.1 eV detection range), and a Si CCD detector (1.1 eV–2.3 eV). The excitation laser wavelength was 532 nm. All spectra were collected at room-temperature as well as at normal incidence in backscattering geometry. A white-body lamp was used to determine the optical response of the setup used for the calibration of the spectra.

μPL measurements were performed at eleven equidistant positions along the radius of the waver from the center to the edge. In all the measurements, we have predominantly

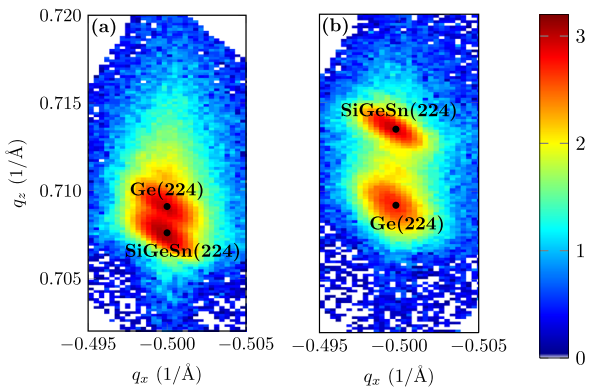

FIG. 2. Reciprocal space map (RSM) of the middle of the wafer for sample A (left panel) and sample B (right panel). The colorbar indicates the intensity of the reflected light on a logarithmic scale.

TABLE II. Comparison between unstrained lattice constants a_{EXP} as calculated from XRD data, lattice constant a_{VEG} calculated according to Vegard's law, and lattice constant a_{EMP} calculated according to Ref. 18. Values in parentheses indicate the deviation from the experimental value in percent.

Sample	a_{EXP} (Å)	a_{VEG} (Å)	a_{EMP} (Å)
A	5.658	5.663 (−0.09)	5.668 (−0.18)
B	5.631	5.640 (−0.15)	5.647 (−0.28)

observed a strong peak around 0.90 eV for both sample A and sample B with a shoulder towards lower energies (see Fig. 3 for representative spectra). We attribute the stronger peak to the direct transition and the low energy shoulder to the indirect gap transition.[21] Optical recombination processes are more efficient for direct band gap transitions and can be expected to lead to a higher PL signal intensity. Furthermore, we can expect the contribution of the indirect transition to the PL signal to be small because of the lack of self-absorption in our thin GeSiSn layers.[22] The signal of the indirect transition is too weak to be quantitatively analyzed. Therefore, we will only concentrate on the stronger direct transition. To extract the peak energy, we fitted the peak with a Gaussian (data shown in Fig. 4). Due to local variations in concentration that cannot be captured by RBS but affects our PL measurements, we see variations in spectral shape and peak positions with the broadening of the direct transition peak most likely due to concentration variations within the μPL sampling volume. Note that we did not observe any μPL-related features in the photon energy region above 1.1 eV.

As a first step to calculate the bowing parameter of the SiSn binary alloy, we corrected the band-gap of the samples for the tensile strain. Using the information about strained and unstrained lattice constants from XRD and applying deformation potential theory for biaxially strained crystals,[29] we can calculate the effects of hydrostatic and shear strain on the band-gap. With this information, we calculated the size of the band-gap for the case of an unstrained crystal. Material parameters used for this calculation are given in Table III. In accordance with the literature[3,30] and our findings on the lattice constant, all material parameters were linearly averaged according to the measured composition. The material composition for each PL data point was calculated by linear interpolation of the RBS data. For sample A

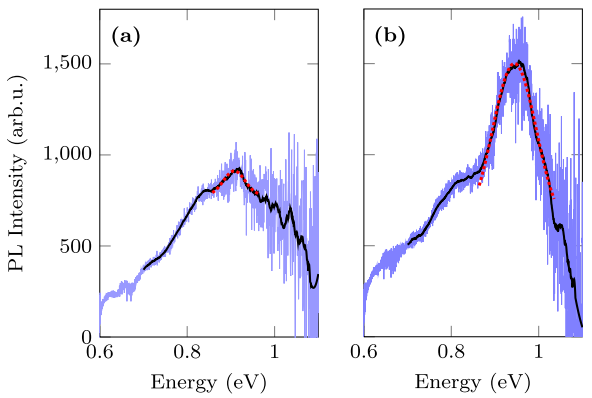

FIG. 3. Examplary photoluminescence spectra of sample A (left panel) and sample B (right panel). Displayed are original data (blue), smoothed data (black), and Gaussian fit (red dashed line).

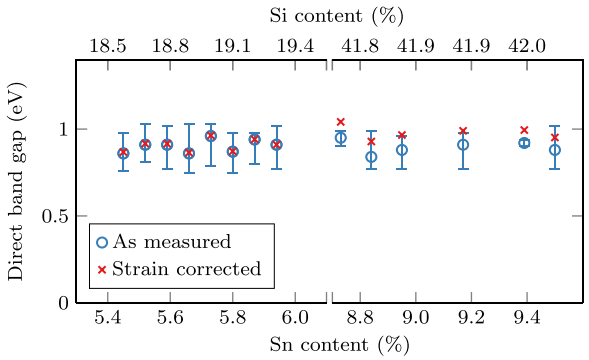

FIG. 4. Direct band-gap as measured by μPL and strain corrected value. The data clustered around low (high) Sn content correspond to sample A (sample B).

(sample B), strain leads, on average, to a decrease of the band-gap by 4 meV (82 meV), see Fig. 4. From the strain corrected band-gap energies, the SiSn bowing parameter was calculated according to Eq. (1). For the band-gaps of the constituent materials Si, Ge, and Sn as well as the SiGe bowing parameter, we followed D'Costa *et al.* and used the values 4.1 eV, 0.8 eV, −0.41 eV, and 0.21 eV, respectively.[11,14] For the GeSn bowing parameters, several values can be found in the literature varying between 1.94 eV and 2.61 eV.[11,31] Here, we use the value of 2.46 eV.[12] However, as will be shown in the following, the bowing behavior of the GeSiSn band-gap is dominated by the SiSn bowing parameter and variations of the GeSn bowing parameter, therefore, have only a minor effect. We performed a two-way analysis calculating the mean value of the bowing parameter for sample A and sample B separately as well as across all samples. For sample A and sample B, we obtain a value of (29 ± 5) eV and (24 ± 4) eV, respectively. The mean value across all samples is (24 ± 2) eV. Within the experimental uncertainties we do not see a concentration dependence of the bowing parameter for our samples. We will, therefore, use the value of (24 ± 2) eV for our further analysis. In Fig. 5(a) we compare our predictions of the composition dependence of the direct band-gap for Ge lattice-matched $Ge_{1-x-y}Si_xSn_y$ alloys with the experimental studies of D'Costa *et al.*[14] and Gallagher *et al.*[9] A significant difference is that D'Costa *et al.* predicted the direct band-gap of $Ge_{1-x-y}Si_xSn_y$ alloys to be always larger than that of pure Ge while, using the result of our experiments, we predict a smaller band-gap for $Ge_{1-x-y}Si_xSn_y$ alloys with a Sn concentration above 12%. This has significant implications when comparing the size of

TABLE III. Material parameters used for the removal of the effects of strain on the valence band (VB) and conduction band (CB) edges of the band gap at the Γ-point.

Parameter	Si	Ge	Sn
Poisson's ratio[a]	0.28	0.27	0.30
Deformation potential VB (eV)[b]	2.38	2.23	1.58
Deformation potential CB (eV)[c]	−10.06	−7.83	−6.00
Shear deformation potential (eV)[d]	−2.1	−2.9	−2.3
Spin-orbit splitting (eV)[a]	0.04	0.29	0.80

[a]Reference 23.
[b]Reference 24.
[c]Reference 25.
[d]References 26–28.

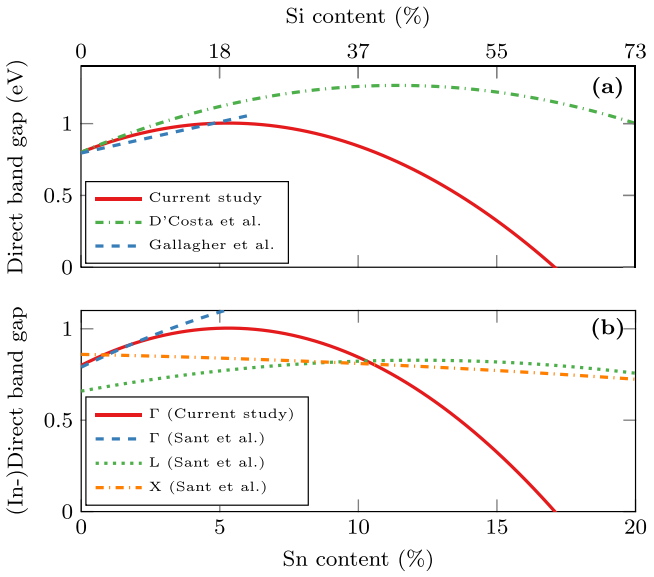

FIG. 5. (a) Prediction of the size of the direct band-gap according to our study (red), D'Costa *et al*. (green), and Gallagher *et al*. (blue dashed line). (b) Comparison of the concentration dependence of the direct band-gap Γ with *X* and *L* indirect band-gaps as computed by Sant *et al*. Both figures assume a Ge lattice-matched $Ge_{1-x-y}Si_xSn_y$ alloy.

the direct band-gap with that of the indirect band-gap as computed by Sant and Schenk[17] using empirical pseudopotentials (see Fig. 5(b)). Following our parametrization of the bowing equation, this would mean that for Sn concentrations of roughly 11%, the lattice-matched $Ge_{1-x-y}Si_xSn_y$ alloy undergoes a transition from indirect to direct band-gap semiconductor. This is in contrast to the predictions of D'Costa *et al*. where $Ge_{1-x-y}Si_xSn_y$ lattice matched to Ge always is an indirect semiconductor. However, both studies overestimate the direct band-gap in comparison to the linear approximation made by Gallagher *et al*. based on $Ge_{1-x-y}Si_xSn_y$ alloys with small Sn and Si concentrations,[9] see Fig. 5(a).

In conclusion, we demonstrated the growth and characterization of $Ge_{1-x-y}Si_xSn_y$ samples closely lattice-matched to Ge with the highest Si concentration measured to date. For all samples, we detected photoluminescence only below 1.1 eV indicating a much stronger band-gap bowing than previously ascribed by theory and experiment. Using a semi-empirical bowing equation based on the band-gaps of the elemental semiconductors and the binary bowing terms, we calculated a SiSn bowing parameter of (24 ± 2) eV. Comparing the predictions for the direct band-gap of Ge lattice-matched $Ge_{1-x-y}Si_xSn_y$ alloys made by three experimental studies, including ours, we found considerable disagreement between them. One possible explanation for this, as already put forward by Beeler *et al*.,[32] is that the bowing parameter b_{SiSn} is either composition-dependent or that higher order terms have to be included in Eq. (1) in order to predict the direct band-gap of $Ge_{1-x-y}Si_xSn_y$ over a broad range of compositions. Therefore, we call for further experiments on $Ge_{1-x-y}Si_xSn_y$ samples that span a greater range of material concentrations. Experimental investigations whether Ge lattice-matched $Ge_{1-x-y}Si_xSn_y$ will indeed turn into a direct band-gap semiconductor for large Sn concentrations would also be very interesting. Finally, strategies to further improve layer quality, e.g., varying growth parameters such as temperature or using a thicker, fully relaxed Ge buffer layer could be investigated.

T.W. and K.B. were supported by the Stiftung der Deutschen Wirtschaft (sdw) and by the Deutsche Forschungsgemeinschaft (DFG) through project B10 within the Collaborative Research Center (CRC) 951 Hybrid Inorganic/Organic Systems for Opto-Electronics.

[1]R. Koerner, M. Oehme, M. Gollhofer, M. Schmid, K. Kostecki, S. Bechler, D. Widmann, E. Kasper, and J. Schulze, Opt. Express **23**, 14815 (2015).
[2]S. Wirths, R. Geiger, N. von den Driesch, G. Mussler, T. Stoica, S. Mantl, Z. Ikonic, M. Luysberg, S. Chiussi, J. Hartmann, H. Sigg, J. Faist, D. Buca, and D. Grützmacher, Nat. Photonics **9**, 88 (2015).
[3]G.-E. Chang, S.-W. Chang, and S. L. Chuang, Opt. Express **17**, 11246 (2009).
[4]G. Sun, R. Soref, and H. Cheng, Opt. Express **18**, 19957 (2010).
[5]I. A. Fischer, T. Wendav, L. Augel, S. Jitpakdeebodin, F. Oliveira, A. Benedetti, S. Stefanov, S. Chiussi, G. Capellini, K. Busch *et al*., Opt. Express **23**, 25048 (2015).
[6]T. Yamaha, S. Shibayama, T. Asano, K. Kato, M. Sakashita, W. Takeuchi, O. Nakatsuka, and S. Zaima, Appl. Phys. Lett. **108**, 061909 (2016).
[7]B. R. Conley, H. Naseem, G. Sun, P. Sharps, and S.-Q. Yu, in *2012 38th IEEE Photovoltaic Specialists Conference (PVSC)* (IEEE, 2012), pp. 001189–001192.
[8]J. Schulze, A. Blech, A. Datta, I. A. Fischer, D. Hähnel, S. Naasz, E. Rolseth, and E.-M. Tropper, Solid-State Electron. **110**, 59 (2015).
[9]J. Gallagher, C. Xu, L. Jiang, J. Kouvetakis, and J. Menéndez, Appl. Phys. Lett. **103**, 202104 (2013).
[10]V. D'Costa, Y.-Y. Fang, J. Tolle, J. Kouvetakis, and J. Menéndez, Thin Solid Films **518**, 2531 (2010).
[11]V. R. D'Costa, C. S. Cook, A. Birdwell, C. L. Littler, M. Canonico, S. Zollner, J. Kouvetakis, and J. Menéndez, Phys. Rev. B **73**, 125207 (2006).
[12]L. Jiang, J. Gallagher, C. Senaratne, T. Aoki, J. Mathews, J. Kouvetakis, and J. Menéndez, Semicond. Sci. Technol. **29**, 115028 (2014).
[13]J. Tolle, A. Chizmeshya, Y.-Y. Fang, J. Kouvetakis, V. DCosta, C.-W. Hu, J. Menendez, and I. Tsong, Appl. Phys. Lett. **89**, 231924 (2006).
[14]V. D'Costa, Y.-Y. Fang, J. Tolle, J. Kouvetakis, and J. Menendez, Phys. Rev. Lett. **102**, 107403 (2009).
[15]H. Lin, R. Chen, W. Lu, Y. Huo, T. I. Kamins, and J. S. Harris, Appl. Phys. Lett. **100**, 141908 (2012).
[16]P. Moontragoon, R. Soref, and Z. Ikonic, J. Appl. Phys. **112**, 073106 (2012).
[17]S. Sant and A. Schenk, Appl. Phys. Lett. **105**, 162101 (2014).
[18]P. Aella, C. Cook, J. Tolle, S. Zollner, A. Chizmeshya, and J. Kouvetakis, Appl. Phys. Lett. **84**, 888 (2004).
[19]G. Capellini, M. De Seta, P. Zaumseil, G. Kozlowski, and T. Schroeder, J. Appl. Phys. **111**, 073518 (2012).
[20]P. Harrison, *Quantum Wells, Wires and Dots: Theoretical and Computational Physics of Semiconductor Nanostructures* (John Wiley & Sons, 2005).
[21]L. Jiang, C. Xu, J. D. Gallagher, R. Favaro, T. Aoki, J. Menéndez, and J. Kouvetakis, Chem. Mater. **26**, 2522 (2014).
[22]M. Virgilio, T. Schroeder, Y. Yamamoto, and G. Capellini, J. Appl. Phys. **118**, 233110 (2015).
[23]O. Madelung, *Semiconductors: Data Handbook* (Springer Science & Business Media, 2004).
[24]Y.-H. Li, X. Gong, and S.-H. Wei, Phys. Rev. B **73**, 245206 (2006).
[25]S.-H. Wei and A. Zunger, Phys. Rev. B **60**, 5404 (1999).
[26]L. D. Laude, F. H. Pollak, and M. Cardona, Phys. Rev. B **3**, 2623 (1971).
[27]M. Chandrasekhar and F. H. Pollak, Phys. Rev. B **15**, 2127 (1977).
[28]B. J. Roman and A. Ewald, Phys. Rev. B **5**, 3914 (1972).
[29]C. G. Van de Walle, Phys. Rev. B **39**, 1871 (1989).
[30]Y.-H. Zhu, Q. Xu, W.-J. Fan, and J.-W. Wang, J. Appl. Phys. **107**, 073108 (2010).
[31]A. A. Tonkikh, C. Eisenschmidt, V. G. Talalaev, N. D. Zakharov, J. Schilling, G. Schmidt, and P. Werner, Appl. Phys. Lett. **103**, 032106 (2013).
[32]R. Beeler, C. Xu, D. Smith, G. Grzybowski, J. Menéndez, and J. Kouvetakis, Appl. Phys. Lett. **101**, 221111 (2012).